≪연구논문≫ The Journal of Optical Society of Korea(Korean Edition) Volume 4, Number 1, March 1993

Transient Behaviour of Photorefractive $Bi_{12}SiO_{20}$ Crystal: Two Wave Mixing with an External A.C. Field

Chong Hoon Kwak and El-Hang Lee
Research Department, Electronics and Telecommunications Research Institute, Taejon, 305-350, Korea

Jeno Takacs and Laszlo Solymar
Holography Group, Department of Engineering Science, University of Oxford, Parks Road, Oxford, OX1 3PJ, U.K.

(Received: January 14, 1993)

The temporal differential equation describing the build-up of the space-charge field in the presence of square and sinusoidal alternating field in photorefractive materials is solved analytically. We also measured the average two-wave mixing gain and the full temopral gain variations in a $Bi_{12}SiO_{20}$ crystal with applied fields of up to 7 KV/cm amplitude and 1 KHz repetition rate. It has been found that the experimental measurements agree well with the theoretical results.

I. INTRODUCTION

Nonlinear optical interaction of two coherent waves giving the interference pattern in photorefractive materials results in versatile interesting phenomena such as optical amplifications,[1,2] phase conjugation,[3] dynamic volume holography,[4-6] and recently observed spatial subharmonic generations.[7-12] Nonlinear energy coupling in photorefractive materials has a wide range of applications because photorefractive media provide unique features like real time operation, high optical gain, storage, nonlinear operation and correlation. These include image amplification,[2,13] vibrational analysis,[14] laser gyros,[15] nonreciprocal transmission,[16] neural network,[17] parallel half-adder circuit,[18] opical correlator,[19] novelty filter,[20] pattern recognition,[21] opitical interconnections[22] and photonic switchings.[23]

Two wave mixing (TWM) gain is one of the most fundamental and attractive aspects of the photorefractive effect. It is used as a tool for understanding and studying material parameters and processes and as a building block for more complex optical systems. Several techniques for the enhancement of TWM gain have been developed and analysed by many researchers; applied d.c. field technique,[24] d.c. field and moving grating technique[25,26] intensity- and temperature-dependent technique,[27] and applied a.c. field technique.[28,29]. It was shown some time ago by Stepanov *et al.*[28] that TWM gain can be considerably increased by applying an a.c. electric field instead of a d.c. field. Under the ideal conditions the optimum gain achievable with an a.c. field is equal to that with a d.c. field accompanied by frequency detuning, i.e., moving grating.

Our work in this paper has been very detailed measuring not only the average (steady state) TWM gain but the full temporal variation of the gain as well including transient phenomena for the square and sinusoidal applied fields in a photorefractive $Bi_{12}SiO_{20}$ crystal. We also developed, for the first time, the corresponding theory based on Kukhtarev's materials equations.[30]

II. PROBLEM FORMULATION

1. Two Wave Mixing Gain.

Considerable effort has been devoted to measure

TWM gain experimentally and describe mathematically the transient energy transfer in a two wave mixing experiment.[31-33] The case when ac field is applied is a special interest, which to our knowledge has not been mathematically modelled.

In a photorefractive crystal the effective gain in a two mixing configuration defined as follows.[13]

$$G=\frac{I_s(\text{with pump beam and AC field})}{I_s(\text{without pump beam and AC field})}$$

$$=\frac{(1+\beta)\exp(\Gamma d)}{1+\beta\exp(\Gamma d)} \tag{1}$$

where $\beta=I_s(0)/I_R(0)$ is the incident intensity beam ratio, I_s (I_R) is the intensity of the probe (pump) beam emerging from the crystal, and d is the interaction length in the crystal. The exponential gain coefficient Γ, which in our case is a time function, is defined in the following form[24]:

$$\Gamma(t)=\frac{2\pi n^3 r_{eff}}{\lambda\cos\theta}\ \frac{|Im\{E_{SC}(t)\}|}{m} \tag{2}$$

where λ is the wavelength, n is the refractive index, r_{eff} is the effective linear electro-optic coefficient (a function of the crystal orientation and incident beam polarization), θ is the Bragg angle in the crystal, m is the fringe modulation and $E_{sc}(t)$ is the transient complex amplitude of the space-charge field. In order to investigate the transients of two wave mixing in photorefractive materials, we need the temporal solution of the space-charge field $E_{sc}(t)$.

2. Space-Charge Field with Applied A.C. Electric Field

Starting with the Kukhtarev's material equations[30] and using the first order perturbation theory, we can obtain, after some algebra, the temporal differential equation describing the build-up of the space-charge field $E_{sc}(t)$ with external applied field $E_o(t)$ in the following form[25]:

$$\frac{\partial E_{SC}}{\partial t}+gE_{SC}=hm \tag{3a}$$

Here, the coefficients are as follows:

$$g=\frac{1-i\dfrac{E_o}{E_q}}{\tau_d\left(1-i\dfrac{E_o}{E_M}\right)} \qquad h=\frac{-E_o}{\tau_d\left(1-i\dfrac{E_o}{E_M}\right)} \tag{3b}$$

where τ_d is the Maxwell relaxation time, $E_M=1/\mu\tau_e K$ and $E_q=eN_A/\varepsilon_o\varepsilon K$, K is the magnitude of the grating wave vector, τ_e is the lifetime of the photoelectrons, N_A is the acceptor density, μ is the mobility and $\varepsilon_o\varepsilon$ is the dielectric constant. For simplicity, in deriving Eq.(3) we neglect the diffusion field, which is small in $Bi_{12}SiO_{20}$ crystal compared with E_q and E_o. It is noted that although Eq.(3) is derived for a d.c. applied field (i.e., E_o=const.), it is still valid for a.c. applied field when the period T $(=2\pi/\Omega)$ of a.c. applied field is much longer than the lifetime of the photoelectrons, i.e., $T\gg\tau_e$. In that case, each photoelectron essentially sees a constant applied field during its lifetime. In addition, when the period of the a.c. field is much shorter than the grating build-up time τ_g (approximately equal to Re{1/g}), one may use the time averaging method over the period T to solve Eq.(3)[28]. Then the space-charge field cannot follow the a.c. applied field and the solution becomes independent of the time period T. When, however, the period T is comparable with τ_g, the usual time averaging method will not hold, so we require to have the full temporal solution for $E_{sc}(t)$, applicable to the whole frequency range of the a.c. field.

III. TRANSIENT SOLUTION FOR SPACE-CHARGE FIELD

1. Square Wave Field

Consider the square a.c. field $E_o(t)$ with the time period $T(=2\pi/\Omega)$ as shown in Fig. 1. Then, the time varying coefficients $g(t)$ and $h(t)$ in Eq.(3) become constants g^+ and h^+ for each positive half-period of $E_o(t)$ $=E_o$, and g^- and h^- for each negative half-period of $E_o(t)=-E_o$, respectively, where E_o is the amplitude of square applied field. In order to solve Eq.(3), we apply the step-by-step integration in each successive half-period of $E_o(t)$. Then the general solution of Eq.(3) is given by

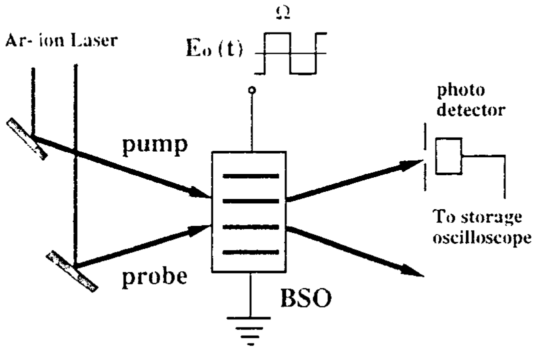

Fig. 1 Experimental setup for measuring two wave mixing gain in photorefractive $Bi_{12}SiO_{20}$ crystal. Alternating electric field of square and sinusoidal field is applied on the crystal.

$$E_n(t)=\exp(-gt)\left[\int_{t_0}^{t}\exp(gt')\,h(t')m\,dt'+C(t_0)\right] \tag{4}$$

where $C(t_o)$ is an integration constant to be determined from the boundary condition at $t=t_o$. Considering the nth period of the applied field $E_o(t)$ (i.e., $(n-1)T\leq t\leq nT$) and using Eq.(4) we get the space-charge field $E_n(t)$ for the positive and the negative half-period as

$$E_n^+(t)=\frac{h^+}{g^+}m\{1-\exp[-g^+(t-(n-1)T)]\}+E_n^+[(n-1)T]$$
$$\times\exp[-g^+(t-(n-1)T)]$$
$$\text{for } (n-1)T\leq t\leq(n-\frac{1}{2})T \tag{5a}$$

$$E_n^-(t)=\frac{h^-}{g^-}m\{1-\exp[-g^-(t-(n-\frac{1}{2})T)]\}+E_n^-[(n-\frac{1}{2})T]$$
$$\times\exp[-g^-(t-(n-\frac{1}{2})T)]$$
$$\text{for } (n-\frac{1}{2})T\leq t\leq nT \tag{5b}$$

From Eq.(3b) we have the following relations: $g^{+*}=g^-$ and $h^{+*}=-h^-$. Before proceeding any further, it is covenient to introduce the steady state values of $E_n(t)$. Since the steady state of $E_n(t)$ corresponds to the values for sufficiently large n, we may take the boundary conditions as

$$E_n^+\left[(n-\frac{1}{2})T\right]=E_n^-\left[(n-\frac{1}{2})T\right]\equiv E_\infty^+ \tag{6a}$$

$$E_n^+[(n+1)T]=E_n^-(nT)\equiv E_\infty^- \tag{6b}$$

where $E_\infty^\pm$ are the steady state values of the space-charge field for the positive and negative half-period, respectively. Substituting now Eq.(6) into Eq.(5) and we get the steady state values of spacecharge field in the following form:

$$E_\infty^+=\frac{1}{1-\exp(-g_{av}T)}\left\{\frac{h^+}{g^+}m[1-\exp(-\frac{g^+}{2}T)]\right.$$
$$\left.+\frac{h^-}{g^-}m[1-\exp(-\frac{g^-}{2}T)]\exp-(\frac{g^+}{2}T)\right\} \tag{7a}$$

$$E_\infty^-=\frac{1}{1-\exp(-g_{av}T)}\left\{\frac{h^-}{g^-}m[1-\exp(-\frac{g^-}{2}T)]\right.$$
$$\left.+\frac{h^+}{g^+}m[1-\exp(-\frac{g^+}{2}T)]\exp(-\frac{g^-}{2}T)\right\} \tag{7b}$$

where $g_{av}=(g^++g^-)/2$. By using the relations $g^{+*}=g^-$ and $h^{+*}=-h^-$, it may easily be seen that $E_\infty^+=-E_\infty^-$. For convenience, we introduce the following notations;

$$E_\infty^\pm=\pm a_\infty+ib_\infty, \tag{8a}$$

$$g^\pm=g_1\pm ig_2, \tag{8b}$$

$$h^\pm=\pm h_1+ih_2, \tag{8c}$$

After simple calculations, we have the frequency-dependent (steady state) space-charge fields as

$$a_\infty(T)=\frac{g_1h_1+g_2h_2}{g_1^2+g_2^2}m\left[\coth\left(\frac{g_1T}{2}\right)-\frac{\cos\left(\frac{g_2T}{2}\right)}{\sinh\left(\frac{g_1T}{2}\right)}\right] \tag{9a}$$

$$b_\infty(T)=\frac{g_1h_2-g_2h_1}{g_1^2+g_2^2}m+\frac{g_1h_1+g_2h_2}{g_1^2+g_2^2}m\frac{\sin\left(\frac{g_2T}{2}\right)}{\sinh\left(\frac{g_1T}{2}\right)} \tag{9b}$$

In the limiting case of $T/2\ll 1/g_{1,2}$ (i.e., for high frequency limit) Eq.(9) reduces to:

$$a_\infty\simeq 0 \tag{10a}$$

$$b_\infty\simeq\frac{h_2}{g_1}m=-\frac{E_oE_q}{E_ME_q+E_o^2}mE_o \tag{10b}$$

which gives the same expression derived by using time averaging method proposed by Stepanov and Petrov.[28] Note that the absolute value of the imaginary part of space-charge field is equal to the value derived from the optimized moving grating technique.[25] Having the expressions for steady state space-charge field $E^{\pm}_{\infty}$, it may be possible to express $E_n(t)$ for an arbitrary nth period of square wave in terms of $a_\infty(T)$ and $b_\infty(T)$. By using the boundary condition of $E^-_n[(n-\frac{1}{2})T]=E^+_n[(n-\frac{1}{2})T]$ and Eq.(7), we get the expression for $E_n^+[(n-1/2)T]$ and $E^-_n(nT)$ in the following form:

$$E^+_n[(n-\frac{1}{2})T]=E^+_\infty-E^-_\infty\exp(-\frac{g^+}{2}T)+E^+_n(n-1)+\exp(-\frac{g^+}{2}T) \tag{11a}$$

$$E_n^-(nT)=E^-_\infty[-\exp(-g_{av}T]+E^+_n[n-1)T]\times\exp(-g_{av}T) \tag{11b}$$

Since $E_n^+[(n-1)T]=E^-_{n-1}[(n-1)T]$, we have the following relations from Eq.(11b) by using successive iterations;

$$E^-_n(nT)=E^-_\infty[1-\exp(-ng_{av}T)] \tag{12a}$$

where $E^-_o(0)=0$ is taken the initial condition. Substituting now Eq.(12a) into Eq.(11a) we have

$$E^+_n[(n-\frac{1}{2})T]=E^+_\infty-E^-_\infty\exp[-(ng_{av}-\frac{g^-}{2})T] \tag{12b}$$

The imaginary part of Eq.(12) gives the overall temporal behavior of the square wave field at the beginning of each half-period.

On substituting Eq.(12) into Eq.(5) we may have the transient solution for each half-period of applied field in the following form.

$$E^+_n(t)=\frac{h^+}{g^+}m[1-\exp(-g^+t)]+E^-_\infty\{1-\exp[-(n-1)\times g_{av}T]\}\exp(-g^+t) \quad \text{for } 0\le t\le\frac{T}{2} \tag{13a}$$

$$E^-_n(t)=\frac{h^-}{g^-}m[1-\exp(-g^-t)]-\{E^+_\infty-E^-_\infty\exp[-(n-1)\times g_{av}T]\}\exp(-g^-t) \quad \text{for } 0\le t\le\frac{T}{2} \tag{13b}$$

where the origin of time is taken to be the beginning of each half-period. This periodic oscillatory behavior is caused by the transient changes in the applied field. Taking the imaginary parts of Eq.(13), after some algebra, we get

$$Im\{E^+_n(t)\}=Im\{E^+_\infty(t)\}-\exp[-g_1(t+(n-1)T)]\times(a_\infty\sin(g_2t)+b_\infty\cos(g_2t)) \quad \text{for } 0\le t\le\frac{T}{2} \tag{14a}$$

$$Im\{E^-_n(t)\}=Im\{E^-_\infty(t)\}+\exp\left\{-g_1[t+(n-\frac{1}{2})T]\right\}\times\left\{\left[a_\infty\cos\left(\frac{g_2}{2}T\right)-b_\infty\sin\left(\frac{g_2}{2}T\right)\right]\sin(g_2t)-\left[a_\infty\sin\left(\frac{g_2}{2}T\right)+b_\infty\cos\left(\frac{g_2}{2}T\right)\right]\cos(g_2t)\right\} \quad \text{for } 0\le t\le\frac{T}{2} \tag{14b}$$

where

$$Im\{E^+_\infty(t)\}=Im\{E^-_\infty(t)\}=b_\infty+\frac{2a_\infty}{1-2\exp(-\frac{g_1}{2}T)\cos(\frac{g_2}{2}T)+\exp(-g_1T)}\times\left\{[1-\exp(-\frac{g_1}{2}T)\cos(\frac{g_2}{2}T)]\exp(-g_1t)\sin(g_2t)-[1-\exp(-g_1t)\cos(g_2t)]\exp(-\frac{g_1}{2}T)sin(\frac{g_2}{2}T)\right\} \quad \text{for } 0\le t\le\frac{T}{2} \tag{14c}$$

Here, $Im[E^{\pm}_\infty(t)]$ *is the change in the space-charge field after its average value reached the steady state (i.e., for* $n\gg1$). Note that $Im[E^+_\infty(t)]=Im[E^-_\infty(t)]$ for each half-period, implying frequency doubling in two wave mixing gain as we shall see later.

2. Sinusoidally Varying Field

In this section we will solve Eq.(3) for sinusoidal field applied to the crystal. Now we assume the solution in the following form:

$$E_o(t)=E_o \sin\Omega t \tag{15a}$$

$$E_{SC}(t)=A_o(t)+\sum_{n=1}^{\infty} A_n(t)\sin(n\Omega t-\phi_n) \tag{15b}$$

where ϕ_n is the phase of the nth harmonics and $\Omega=2\pi/T$ is the frequency of the applied field. It is also assumed that the Fourier series of the space-charge field rapidly converges, therefore only the first few terms give a significant contribution to the solution (i.e., $|A_n|\gg|A_{n+1}|$ for $\forall\, n$). At first, we choose an approximate solution in the form

$$E_{SC}(t)=A_o(t)+A_1(t)\sin(\Omega t-\phi_1) \tag{16}$$

Substituting Eq.(16) in Eq.(3) and equating the coefficients of $\cos\Omega t$, $\sin\Omega t$ and constant terms on both sides of the equation, we have

$$\Omega A_1\cos\phi_1-\left(\frac{\partial A_1}{\partial t}+\frac{A_1}{\tau_d}\right)\sin\phi_1=0 \tag{17a}$$

$$\left(\frac{\partial A_1}{\partial t}+\frac{A_1}{\tau_d}\right)\cos\phi_1+\Omega A_1\sin\phi_1=i\left(\frac{E_o}{E_M}\frac{\partial A_o}{\partial t}+\frac{E_o}{E_q}\frac{A_o}{\tau_d}\right)-m\frac{E_o}{\tau_d} \tag{17b}$$

$$i\left(\frac{E_o}{2E_M}\frac{\partial A_1}{\partial t}+\frac{E_o}{2E_q}\frac{A_1}{\tau_d}\right)\cos\phi_1+i\frac{\Omega E_o}{2E_M}A_1\sin\phi_1=\frac{\partial A_o}{\partial t}+\frac{A_o}{\tau_d} \tag{17c}$$

Rewriting Eq.(17a) for $\partial A_1/\partial t$ and inserting this into Eq.(17b) and (17c), we have

$$A_1=\frac{\sin\phi_1}{\Omega}\left[i\left(\frac{E_o}{E_M}\frac{\partial A_o}{\partial t}+\frac{E_o}{E_q}\frac{A_o}{\tau_d}\right)-m\frac{E_o}{\tau_d}\right] \tag{18a}$$

$$\frac{\partial A_o}{\partial t}+\frac{A_o}{\tau_d}=i\left[\frac{E_o}{2E_M}\left(\frac{\Omega}{\sin\phi_1}-\frac{\cos\phi_1}{\tau_d}\right)+\frac{E_o}{2E_q}\frac{\cos\phi_1}{\tau_d}\right]A_1 \tag{18b}$$

For steady state case, Eq.(17a) gives the following relations

$$\sin\phi_1=\frac{b}{\sqrt{1+b^2}},\qquad \cos\phi_1=\frac{1}{\sqrt{1+b^2}} \tag{19}$$

where $b=\Omega\tau_d$ is the dimensionless frequency of a.c. field. After eliminating A_1 from Eq.(8) and substituting Eq.(19) we get the first order differential equation for A_o in the following form.

$$\frac{\partial A_o}{\partial t}+g_{eff}A_o=h_{eff}m \tag{20a}$$

where

$$g_{eff}=\frac{1}{D\tau_d}\left(1+\frac{b^2}{1+b^2}\frac{E_o^2}{2E_qE_M}+\frac{1}{1+b^2}\frac{E_o^2}{2E_q^2}\right) \tag{20b}$$

$$h_{eff}=-\frac{i}{D\tau_d}\left(\frac{b^2}{1+b^2}\frac{E_o^2}{2E_M}+\frac{1}{1+b^2}\frac{E_o^2}{2E_q}\right) \tag{20c}$$

$$D=1+\frac{b^2}{1+b^2}\frac{E_o^2}{2E_M^2}+\frac{1}{1+b^2}\frac{E_o^2}{2E_qE_M} \tag{20d}$$

The solution of Eq.(20) is given by

$$A_o(t)=A_o(\infty)[1-\exp(-g_{eff}t)] \tag{21}$$

where $A_o(\infty)=mh_{eff}/g_{eff}$. It may be noted that g_{eff} is real, so ther is no overshoot or damping in space-charge field. $A_o(\infty)$ is also pure imaginary, which means that the space-charge field, at least A_o, is spatially $\pi/2$ out of phase with respect to the intensity fringe distribution. This represents the optimum phase shift for energy exchange in two wave mixing. For the limit of $b\gg1$, we get

$$A_o(\infty)=\simeq -i\frac{\dfrac{E_o}{2E_M}}{1+\dfrac{E_o^2}{2E_qE_M}}mE_o \tag{22}$$

It may be note that Eq.(22) for sinusoidal field is comparable with Eq.(10) for square wave field. By inserting Eq.(21) into Eq.(18a) we may have the first harmonic amplitude $A_1(t)$ which is rather complicated. However, if one may assume that $Eq\gg E_o\gg E_M$ we have a simple solution in the form;

$$A_1(t)=-\frac{mE_o}{\sqrt{1+b^2}}m\frac{1}{1+\dfrac{b^2}{1+b^2}\dfrac{E_o^2}{2E_ME_q}}\times[1-\exp(-g'_{eff}t)] \tag{23}$$

where

$$g'_{eff}=\left(1+\frac{b^2}{1+b^2}\frac{E_o^2}{2E_ME_q}\right)/D'\tau_d \text{ and } D'=1+\frac{b^2}{1+b^2}\frac{E_o^2}{2E_M^2}$$

For $A_1(t)$ real, it does not contribute to the two wave mixing gain. Furthermore, $A_1(t)$ gradually disappears as b grows (i.e., in the high frequency range $A_1(t)$ may be negligible). So, we need to have the second harmonic amplitude $A_2(t)$ for explaining the periodic transient changes of the space-charge field. Considering the second harmonic component $A_2(t)$ in the assumed solution, Eq.(16), and equating the coefficients of $\cos 2\Omega t$ and $\sin 2\Omega t$ terms on both sides of the equation we have

$$2\Omega A_2\cos\phi_2-\left(\frac{\partial A_2}{\partial t}+\frac{A_2}{\tau_d}\right)\sin\phi_2 = -i\frac{E_o}{2E_M}\left(\frac{\partial A_1}{\partial t}\cos\phi_1+\Omega A_1\sin\phi_1\right) \tag{24a}$$

$$\left(\frac{\partial A_2}{\partial t}+\frac{A_2}{\tau_d}\right)\cos\phi_2+2\Omega A_2\sin\phi_2 = -i\frac{E_o}{2E_M}\left(\frac{\partial A_1}{\partial t}\sin\phi_1-\Omega A_1\cos\phi_1\right) \tag{24b}$$

It is obvious from Eq.(24) that $A_2(t)$ is pure imaginary for real A_1 values. For steady state case, Eq.(24) gives the relations

$$\sin\phi_2=\frac{3b}{\sqrt{(1+b^2)(1+4b^2)}},\quad \cos\phi_2=\frac{1-2b^2}{\sqrt{(1+b^2)(1+4b^2)}} \tag{25}$$

Multiplying Eq.(24a) by $\cos\phi_2$ and Eq.(24b) by $\sin\phi_2$, and adding them together we have

$$A_2(t)=-i\frac{E_o}{2E_M}\frac{1}{2\Omega\sqrt{1+4b^2}}\left(\frac{\partial A_1}{\partial t}-2b\Omega A_1\right) \tag{26}$$

For $E_o \gg E_M$, Eq.(26) simply reduces to

$$A_2(t)=-im\frac{\frac{E_o^2}{2E_M}}{1+\frac{b^2}{1+b^2}\frac{E_o^2}{2E_M E_q}}\frac{b}{\sqrt{(1+b^2)(1+4b^2)}} \times[1-\exp(-g'_{eff}t)] \tag{27}$$

Hence, the total space-charge field, which contributes to two wave mixing gain may be expressed as

$$Im\{E_{SC}(t)\}=Im\{A_o(t)+A_2(t)\ \sin(2\Omega t-\phi_2)\} \tag{28}$$

where $\phi_2=\tan^{-1}\frac{3b}{1-2b^2}$

Equation(28) describes the full temporal behavior of the two wave mixing gain at least to the second order approximation, and also depicts the doubling of the applied frequency Ω in the temporal solution. Since the amplitudes of the Fourier series for the space-charge field rapidly converges, one may expects that the higher order components in Eq.(28) do a little affects to the higher harmonics in frequencies.

IV. EXPERIMENTS AND DISCUSSION

The full temporal variation of the two wave mixing (TWM) gain is measured in photorefractive $Bi_{12}SiO_{20}$ crystal grown by Sumitomo ($10\times10\times10$ mm^3). The experimetal configuration is schematically shown in Fig. 1. A beam from an Ar-ion laser at 514.5 nm wavelength was split into two beams, expanded and collimated. The intensity beam ratio of pump-to-probe beams set to 45 with a total incident intensty of 4.6 mW/cm^2. The two beams were vertically polarized and were incident on the (110) face of the BSO crystal. The alternating electric field (square or sinusoidal wave) of up to 7 KV/cm amplitude was applied between the (001) faces of the crystal. The interbeam angle betwen the two incident beams was chosen so as to achieve the optimum gain in experiments at approximately 2° for both a.c. square and sinusoidal applied field, resulting in grating spacing of 15 μm. The temporal evolution of the grating was measured by a photodetector connected to a digital storage oscilloscope and to a X-Y recorder. The frequency range of the applied electric field was 10 Hz~1 KHz. Fig. 2 shows the theoretical curves for temporal behavior of the grating for square wave field of $E_o=7$ KV/cm amplitude with repetition rates of 20, 150, and 800 Hz, respectively. For the various frequencies the three curves show somewhat different features. It may be seen that as time increases the gain oscillates with twice frequency and as the repetition rate increases the oscillatory amplitude rapidly decreases, and eventually drops to zero. In the calculations we used the following crystal parameters: $E_M=0.35$ KV/cm, grating spacing of 15 μm and $\tau_d=1.3$ msec

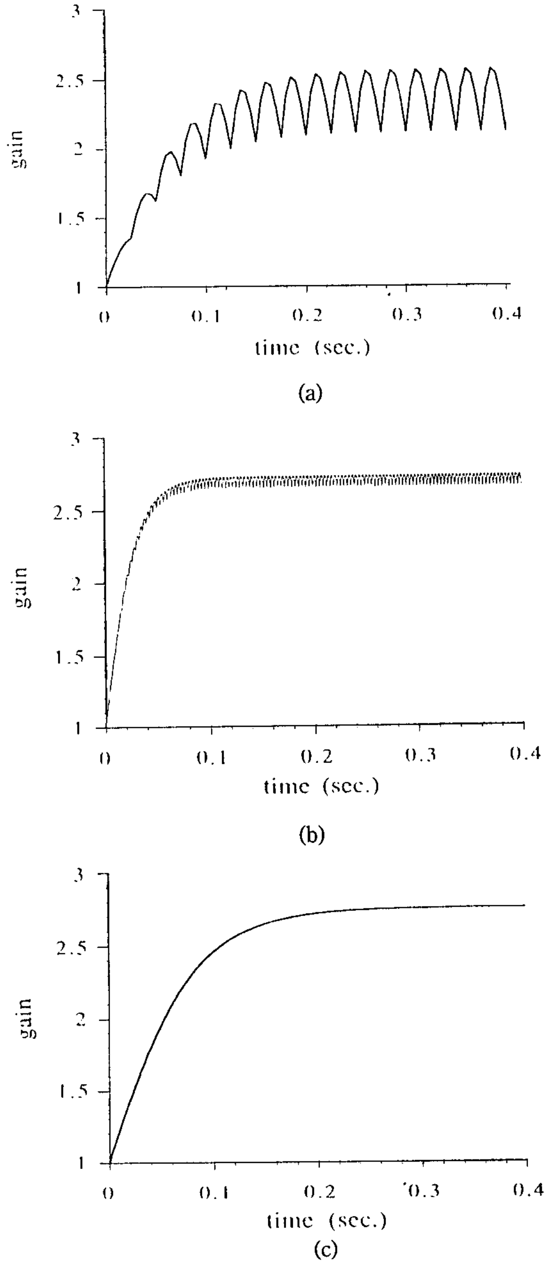

Fig. 2. Theoretical curves for temporal variations of two wave mixing gain in the presence of square a.c. field of 7 KV/cm. The applied frequency is (a) 20 Hz, (b) 150 Hz, and (c) 800 Hz.

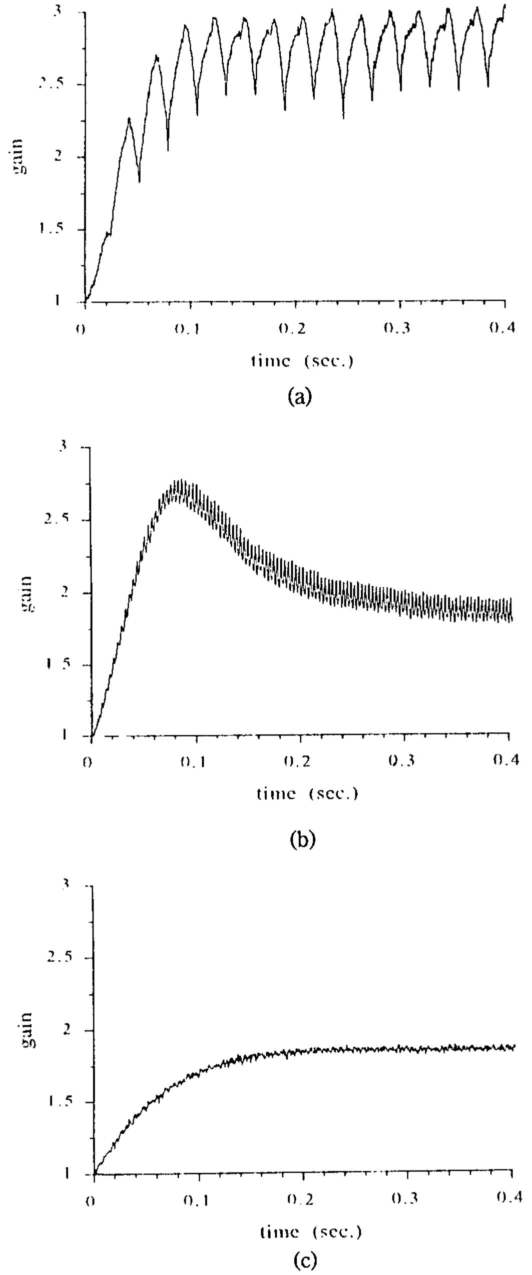

Fig. 3. Experimental verifications of Fig. 2. Square wave field of 7 KV/cm is applied. (a) 20 Hz, (b) 150 Hz, and (c) 800 Hz.

for input intensity of 4.6 mW/cm^2 and g_1=14.7 Hz and g_2=37.7 Hz for E_o=7 KV/cm. Note that these physical parameters listed here are in good agreement with those of the literatures.[10,11,25] Fig. 3 shows the experimental curves for the time-dependent behaviour of TWM gain for the same repetition rates of 20, 150 and 800 Hz, respectively. The theory agrees well with

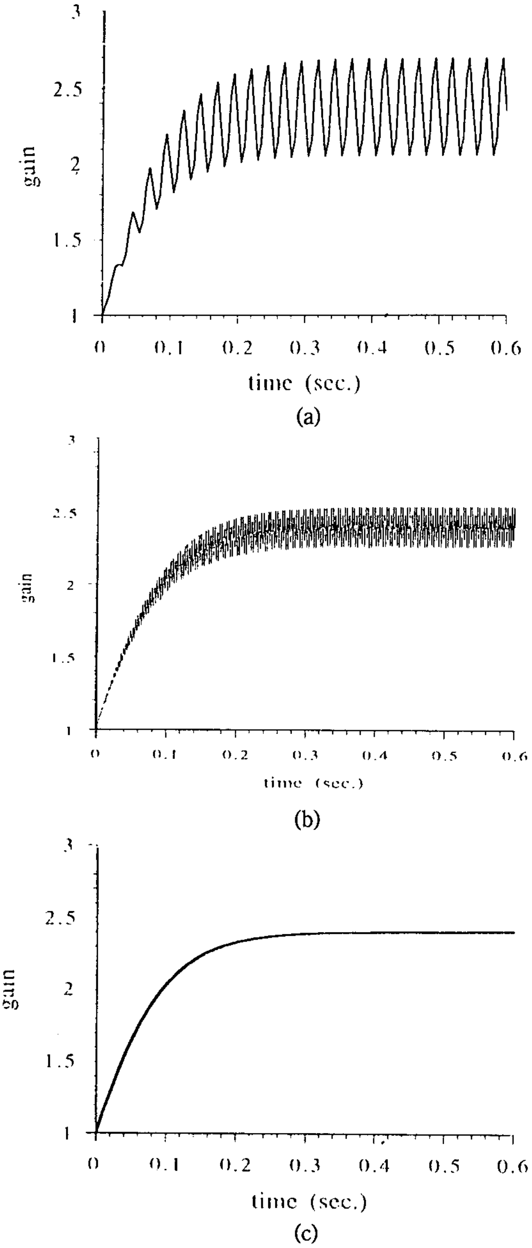

Fig. 4. Theoretical curves for temporal variations of two wave mixing gain in the presence of sinusoidal a.c. field of 7 KV/cm. The applied frequency is (a) 20 Hz, (b) 150 Hz, and (c) 800 Hz.

the experimental results with the exception of one aspect. The experiments show an overshoot in the transient response whereas the theory predicts a monotonic growth. We belive that improved agreement could

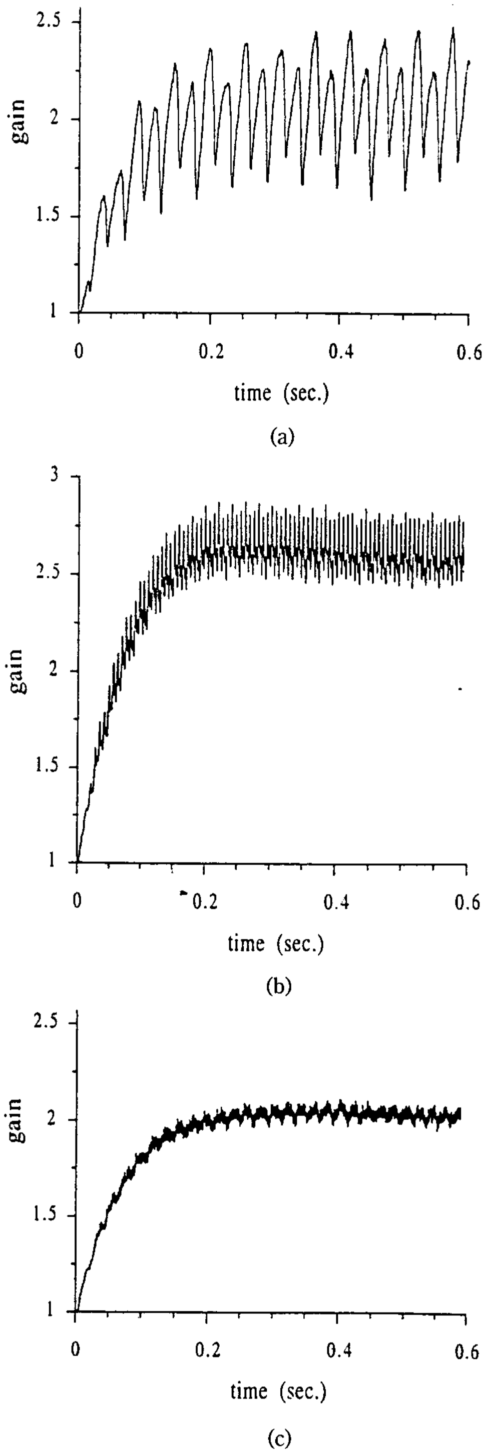

Fig. 5. Experimental verifications of Fig. 4. Sinusoidal wave field of 7 KV/cm is applied. (a) 20 Hz, (b) 150 Hz, and (c) 800 Hz.

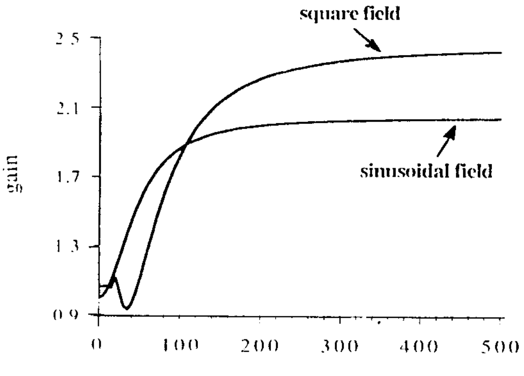

Fig. 6. Theoretical curves of two wave mixing gain as a function of applied frequency for square and sinusoidal electric field of 5 KV/cm.

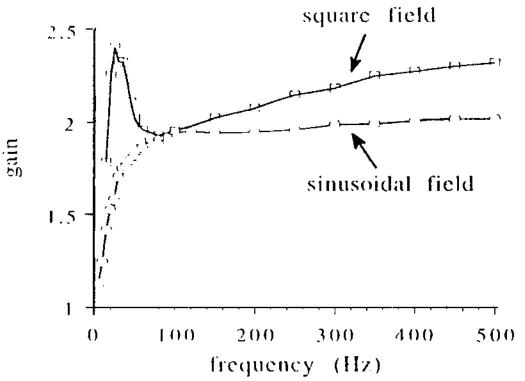

Fig. 7. Experimental verifications of Fig. 6. Square and sinusoidal electric field of 5 KV/cm is applied on the crystal.

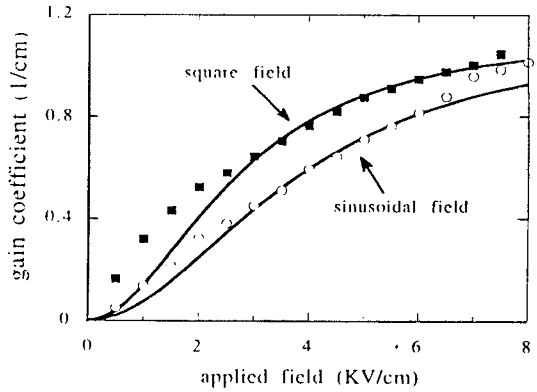

Fig. 8. Optimum two wave mixing gain as a function of applied field for square and sinusoidal electric field. The applied frequency is fixed at 500 Hz. Solid curve is a theoretical curve.

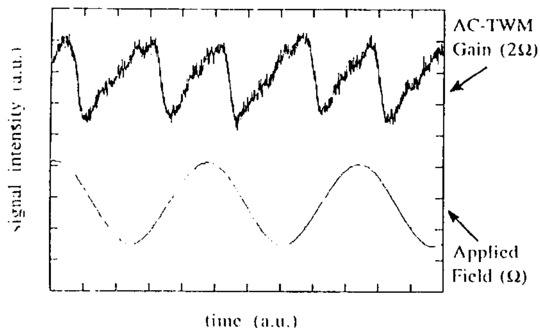

Fig. 9. Photograph of frequency doubling observed in two wave mixing gain experiment.

be obtained by solving simultaneously the materials and the field equations together.[31,32] Fig. 4 shows the theoretical curves for the TWM gain for sinusoidal field of E_o=7 KV/cm amplitude for the same three repetition rates. In calculating the responses shown in Fig. 4 we used the same crystal parameters as before. Fig. 5 represents the experimental verification of the calculated results shown in Fig. 4. The overall behavior is in good agreement with the theory as before. Fig. 6 shows the theoretical curves of TWM gain as a function of the frequency for the square wave and sinusoidal field excitation. It may be seen from Fig. 6 that there is no resonance in TWM gain unlike in the moving grating method.[25] Fig. 7 shows the dependence of the gain on the frequency of square wave and sinusoidal field at E_o=5 KV/cm. Fig. 8 depicts the optimum TWM gain coefficient versus applied field measured at the highest practical frequency, namely 500 Hz. From the best fit with experimental results we obtained the following parameter values: E_q=21 KV/cm, E_M=0.35 KV/cm for K=4.2×10^3 cm^{-1}, r_{eff}=0.28 pm/V, and τ_d=1.5 msec, which is consistent with the value obtained in the case of the square wave field as in Fig. 2 and is again in reasonable agreement with the literature.[10,11,25] Fig. 9 shows the photograph of the double repetition frequency after the gain reached the steady state as predicted in the theory. The wave form of frequency doubling in Fig. 9 shows a rather asymmetric, which means TWM gain contains higher harmonics in frequency.

V. CONCLUSION

We have developed a theory, based on the Kukhtarev's materials equations, describing the temporal variations of two wave mixing gain in the presence of a square and sinusoidal a.c. field in photorefractive materials. The transient behavior of the two wave mixing gain as well as the average (steady state) gain is measured in photorefractive $Bi_{12}SiO_{20}$ crystal for low, medium and high frequency limits (20, 150 and 800 Hz, respectively) with a.c. applied field of up to 7 KV/cm. The experiments are in good agreement with the theory. We expect that the theory developed in this paper could be applicable to another photorefractive materials.

ACKNOWLEDGMENT

This work was performed jointly under the agreement between the University of Oxford and ETRI, and has been supported partly by the Science and Engineering Research Council of Britain and partly by the Minstry of Science and Technology of Korea.

REFERENCE

[1] V. L. Vinetskii, N. V. Kukhtarev, S. G. Odulov, and M. S. Soskin, Sov. Phys. Usp. **22**, 742 (1979).
[2] Y. Fainman, E. Klancnik, and S. H. Lee, Opt. Eng. **25**, 228 (1986).
[3] J. Feinberg, Phys. Today **41** (10), 46 (1988).
[4] P. Gunter and J. P. Huignard, eds., *Photorefractive Materials and Their Applications I* (Springer-Verlag, New York, 1988).
[5] P. Yeh, IEEE J. Quantum Electron. **QE-25**, 484 (1989).
[6] C. H. Kwak, S. Y. Park, H. K. Lee, and E.-H. Lee, Opt, Commun. **79**, 349 (1990).
[7] S. Mallick, B. Imbert, H. Ducollet, J. P. Herriau and J. P. Huignard, J. Appl. Phys. **63**, 5660 (1988).
[8] D. C. Jones and L. Solymar, Opt. Lett. **14**, 743 (1989).
[9] D. J. Webb and L. Solymar, Opt. Commun. **74**, 386 (1990).
[10] C. H. Kwak, J. Takacs, and L. Solymar, Electron. Lett. **28**, 530 (1992).
[11] C. H. Kwak, J. Takacs, and L. Solymar, Opt. Commun. **96**, 278 (1993).
[12] C. H. Kwak, M. Shamonin, J. Takacs, and L. Solymar, Appl. Phys. Lett. **62**, 328 (1993).; C. H. Kwak, M. Shamonin, J. Takacs, and L. Solymer, Opt. Soc. Am. Annual Meeting, MO2 (Albuquerque, New Mexico, 1992).
[13] J. P. Huignard and A. Marrackchi, Opt. Commun. **38**, 249 (1981).
[14] J. P. Huignard and A. Marrackchi, Opt. Lett. **6**, 622 (1981).
[15] P. Yeh, Opt. Commun. **45**, 323 (1983).
[16] P. Yeh, Appl. Opt. **23**, 2974 (1984).
[17] J. H. Hong, S. Campbell, and P. Yeh, Appl. Opt. **29**, 3019 (1990).
[18] H. Rajbenbach, J. Appl. Phys. **62**, 4675 (1987).
[19] H. Rajbenbach *et al.,* Appl. Opt. **31**, 5666 (1992).
[20] D. Z. Anderson and J. Feinberg, IEEE J. Quantum Electron. **QE-25**, 635 (1989).
[21] A. E. Chiou and P. Yeh, Opt. Eng. **27**, 386 (1988).
[22] D. Z. Anderson and D. M. Lininger, Appl. Opt. **26**, 5031 (1987).
[23] S. Weiss, M. Segev, S. Sternklar and B. Fischer, Appl. Opt. **27**, 3422 (1988).
[24] G. C. Valley, J. Opt. Soc. Am. **B1**, 868 (1984).
[25] P. Refregier, L. Solymar, H. Rajbenbach, and J. P. Huignard, J. Appl. Phys. **58**, 45 (1985).
[26] B. Imbert, H. Rajbenbach, S. Mallick, J. P. Herriau and J. P. Huignard, Opt. Lett. **13**, 327 (1988).
[27] G. Picoli, P. Gravey, and C. Ozkul, Opt. Lett. **14**, 1362 (1989).
[28] S. I. Stepanov and M. P. Petrov, Opt. Commun. **53**, 292 (1985).
[29] J. Kumar, G. Albanese, W. H. Steier, and M. Ziari, Opt. Lett. **12**, 120 (1987).
[30] N. Kukhtarev, V. B. Markov, S. G. Odulov, M. S. Soskin, and V. L. Vinetskii, Ferroelectrices **22**, 949 (1979).
[31] T. M. Heaton and L. Solymar, Opt. Acta. **32**, 397 (1985).
[32] N. Kukhtarev, V. B. Markov and S. G. Odulov, Opt. Commun. **23**, 338 (1977).
[33] H. Rajbenbach *et al.*, Opt. Commun. **48**, 247 (1983).

A.C. 전장이 인가된 광굴절 $Bi_{12}SiO_{20}$ 결정의 2광파 혼합 이득의 시간종속 변화

곽종훈 · 이일항
한국전자통신연구소 기초기술연구부

Jeno Takacs and Laszlo Solymar
Holography Group, Department of Engineering Science, University of Oxford, Parks Road, Oxford, OX1 3PJ, U.K.

(1993년 1월 14일 받음)

광굴절결정에 구형파 및 정현파형의 외부 전장을 인가할 때 유기되는 공간 전하장의 시간 종속 해를 해석적으로 유도하였다. $Bi_{12}SiO_{20}$ 결정에 최대 7 KV/cm (주파수<1 KHz)의 전장을 가하면서 시간 종속적인 2광파 혼합의 이득 변화를 측정하고 이론치와 정량적으로 비교 분석하였다.